Volterra Filters for Perceptual Edge Extraction

Stefan Thurnhofer

Dept. of Electrical and
Computer Engineering
University of California
Santa Barbara, CA 93106
e-mail: thurn@agni.ece.ucsb.edu

Sanjit K. Mitra

Dept. of Electrical and
Computer Engineering
University of California
Santa Barbara, CA 93106
e-mail: mitra@ece.ucsb.edu

Abstract

We investigate a class of quadratic Volterra filters, which can be used as computationally efficient edge detectors. Filters from this class are approximately equal to mean-weighted highpass filters, and therefore, they extract fewer edges from dark areas, which is a desirable property for many image enhancement applications. We study the one-dimensional case first and then generalize the results to two dimensions. Since the four-dimensional frequency response yields little insight in the properties of these filters, we also develop a technique for characterizing these filters in a more intuitive way. Using the observation that they map sinusoidal inputs to constant outputs, we employ two-dimensional oriented sinusoids to assess both the frequency characteristics and the degree to which a filter is isotropic, i.e., independent of the input orientation.

1 Introduction

Edge extraction is an important step in many image processing application. In most cases, linear operators similar to the Laplacian-of-Gaussian or the Sobel filter are applied to the image. Thresholding this output or detecting zero-crossings results in a binary image that can be used in computer vision, image registration, etc. Some applications do not need the binarization step and use the filter output directly. One particular example for this case is image contrast enhancement called unsharp masking where a highpass filtered version of the original image is added back to the original image to enhance edges. The goal of this application is to improve the *perceptual* impression of the image and the enhancement has to take into account the properties of the human visual system. One important characteristic is described by Weber's law and it can roughly be stated that noise is more easily perceivable in dark image areas. Therefore, the enhancement must be adapted to the local average grey level.

In this paper, we derive a class of quadratic Volterra filters [1] which are approximately equivalent to mean weighted highpass filters. Because they are also computationally very simple, they are well suited for image enhancement. The analysis of these filters is more intuitive for the one-dimensional case, which we will consider first.

2 Definitions

The basic structure of one-dimensional discrete-time quadratic Volterra filters is given by [2]

$$y(n) = \sum_{k_1=-\infty}^{\infty} \sum_{k_2=-\infty}^{\infty} h_2(k_1, k_2) x(n-k_1) x(n-k_2) \quad (1)$$

where $x(n)$ and $y(n)$ are the input and output sequences, respectively, and $h_2(n_1, n_2)$ is called the generalized impulse response or, for simplicity, impulse response. Similar to linear FIR filters, which combine individual samples, Volterra filters work on products of samples. In this sense, they are a straightforward extensions of the linear case. We restrict ourselves to second-order filters only, since they represent a reasonable trade-off between the advantages of a nonlinear filter and the complexity of design and implementation. The two-dimensional Fourier transform of $h_2(n_1, n_2)$ is defined as the frequency response $H_2(\omega_1, \omega_2)$. Of course, the interpretation of this function is somewhat different than for linear filters and various approaches have been published [3]–[5]. This characterization, however, is not specific enough for our problem, and we will follow a different idea in Section 5. We can easily derive the relationship between input and output spectrum as [3, 6]

$$Y(\omega) = \frac{1}{2\pi} \int_0^{2\pi} H_2(\omega_1, \omega - \omega_1) X(\omega_1) X(\omega - \omega_1)\, d\omega_1, \quad (2)$$

where $X(\omega)$ and $Y(\omega)$ represent the Fourier transforms of $x(n)$ and $y(n)$, respectively. A one-dimensional second-order impulse response is symmetric, if $h_2(n_1, n_2) =$

This work was supported by the SDIO/IST managed by the Office of Naval Research under contract ONR N00014-85-K-0551 and by a University of California MICRO grant with matching funds from Tektronix, Inc., Rockwell International Corporation and Digital Instruments, Inc.

$h_2(n_2, n_1)$. Since every kernel can be transformed into a symmetric response, we will always assume a symmetric kernel. On the other hand, a one-dimensional quadratic *system* is symmetric, if samples before and after the current sample are treated equally, i.e., if $x(n + n_0)$ with $n = 0, 1, \ldots$ has the same influence on the overall result as $x(n - n_0)$.

3 One-Dimensional Filters

In [7], a simple Volterra filter called "Teager's algorithm" was defined: $y(n) = x^2(n) - x(n-1)x(n+1)$. It has been shown that it can be approximated as a mean-weighted highpass filter $y(n) \approx \mu_x(2x(n) - x(n-1) - x(n+1))$, where μ_x represents the local mean of $x(n)$ [8]. However, it was not clear, whether or not these filters would be optimal in any way or which general class of Volterra filters they belong to. We can answer the latter question for one-dimensional filters with the following theorem:

Theorem 1 *A one-dimensional second-order Volterra filter can be approximated by a mean-weighted highpass filter, i.e.,*

$$Y(\omega) \approx 2\mu_x X(\omega) H_2(\omega, 0), \tag{3}$$

if $H_2(\omega, 0)$ has highpass characteristics and

$$H_2(0,0) = \sum_{k_1} \sum_{k_2} h_2(k_1, k_2) = 0 \tag{4}$$

$$H_2(\omega, 0) = H_2(0, \omega) \tag{5}$$

and

$$\begin{aligned} \mathcal{S}^h = & \sum_{\substack{k_1 \\ k_1 \neq k_2}} \sum_{k_2} h_2(k_1, k_2)[2h_2(k_1, k_1) + h_2(k_2, k_2)] \\ & + \sum_{\substack{k_1 \\ k_1 \neq k_2 \\ k_2 \neq k_3}} \sum_{\substack{k_2 \\ k_1 \neq k_2 \\ k_2 \neq k_3}} \sum_{k_3} h_2(k_1, k_2)\Big[h_2(k_1, k_3) + h_2(k_2, k_3)\Big] \\ & \geq 0. \end{aligned} \tag{6}$$

The proof of Theorem 1 is given in [3]. The basic idea is to decompose the general expression of quadratic Volterra filters given in Eq. (1) into the two terms

$$\begin{aligned} y_1(n) &= \mu_x \sum_{k_1} \sum_{k_2} h_2(k_1, k_2)[\hat{x}(n - k_1) + \hat{x}(n - k_2)] \\ y_2(n) &= \mathcal{V}(\hat{x}) \\ &= \sum_{k_1} \sum_{k_2} h_2(k_1, k_2)\hat{x}(n - k_1)\hat{x}(n - k_2) \end{aligned}$$

where $\hat{x}(n) = x(n) - \mu_x$ is the mean-removed version of $x(n)$. Then, we show under which conditions $y_2(n)$ can be neglected compared with $y_1(n)$.

We need to make some remarks about Theorem 1. First, we implicitly assume here and in the following that the input signal's (positive) mean is larger than its variance, which is the case for practically all images and which can always be achieved by appropriate scaling before processing. Second, we can approximate the mean μ_x in Eq. (3) by a local averaging filter, if we assume that the kernel of the Volterra filter is finite. In this case, only pixels in a local neighborhood influence the result, and thus only the local characteristics of the signal play a role for the computation of the output. Third, the assumption that $H_2(\omega, 0)$ has highpass properties is not necessary in general. Even though this is important for edge extraction, any filter for which Eqs. (4) – (6) are true, can be approximated as a mean-weighted filter. For the most general case, we can relax the restrictions even further and drop the symmetry condition in Eq. (5), but then we must rewrite Eq. (3) as

$$Y(\omega) \approx \mu_x X(\omega)[H_2(\omega, 0) + H_2(0, \omega)].$$

We will see, however, that the symmetry condition is automatically fulfilled for important subclasses of mean-weighted highpass filters. Therefore, the only truly necessary conditions are given in Eqs. (4) and (6), which are both written as conditions on the kernel. Even though Eq. (6) appears fairly complicated, we can greatly simplify it for certain special cases, which we call class I and class II. In the first class, filters consist of squares of pixels. The following theorem states the approximate behavior of class I systems.

Theorem 2 *If $h_2(k_1, k_2) = 0$ for all $k_1 \neq k_2$ and $\sum_{k_1} \sum_{k_2} h_2(k_1, k_2) = 0$ and $H_2(\omega, 0)$ has highpass characteristics, then the system can be approximated as a mean-weighted highpass filter.*

Proof: Equation (4) holds by assumption and Eq. (5) is true, since we have $h_2(n_1, n_2) = \sum_k h_2(k, k)\delta(n_1 - k, n_2 - k)$, which leads to $H_2(\omega_1, \omega_2) = \sum_k h_2(k, k)e^{-jk\omega_1 - jk\omega_2}$ and thus $H_2(\omega, 0) = \sum_k h_2(k, k)e^{-jk\omega} = H_2(0, \omega)$.

It remains to show that $\mathcal{S}^h \geq 0$. In the definition for $\mathcal{S}^h$ in Eq. (6) all the sums yield zero because $h_2(k_1, k_2)$ is nonzero only for $k_1 = k_2$. Therefore, we obtain $\mathcal{S}^h = 0$ here. □

The second family of filters is more important for our applications. We call them class II mean-weighted highpass filters (or, short, class II filters) and their mean-weighted highpass property is stated in the following theorem.

Theorem 3 *If $h_2(k_1, k_2) = 0$ for all $k_1 \neq -k_2$ and $\sum_{k_1} \sum_{k_2} h_2(k_1, k_2) = 0$ and $H_2(\omega, 0)$ has highpass characteristics, then the system can be approximated as a mean-weighted highpass filter.*

Proof: Here, we can again simplify $\mathcal{S}^h$ by substituting $k_2 = -k_1$, and with the symmetry condition of $h_2(n_1, n_2)$,

we obtain

$$\mathcal{S}^h = \sum_{\substack{k \\ k \neq 0}} h_2^2(k, -k) \geq 0.$$

In a similar fashion as in the proof of Theorem 1, we can show that

$$H_2(\omega_1, \omega_2) = h_2(0,0) + 2\sum_{k=1}^{\infty} h_2(k, -k)\cos(k\omega_1 - k\omega_2). \tag{7}$$

and thus, $H_2(0, \omega) = H_2(\omega, 0)$ □

The Teager filter is an example for a simple system from this class. It maps sinusoidal inputs to constant outputs, and it is straightforward to show that in fact every class II system has this property. Using Eq. (7), we can see that $H_2(\omega, \omega) = \sum h_2(k, -k) = H_2(0,0)$, which is assumed to be zero, and therefore the output spectrum in Eq. (2) is a single δ-function at $\omega = 0$.

4 Two-Dimensional Filters

We now consider the extension of the previous results to two-dimensional signals for applications in image processing. Since the class II filters of Theorem 3 inherently lead to symmetric systems, we find them very useful for our case. When processing digital images, it is a well-known fact that phase distortion can show up very easily. For linear filters, this means that we desire to use only zero-phase or linear-phase filters, which preserve the original phase information. A constant shift that is induced by linear-phase filters can usually be tolerated.

The fundamental building block of class II systems is $x(n-k)x(n+k)$. The overall system consists of a linear combination of several of these terms for different k. Thus, each term is a product of samples that are equally far away to the left and right of the center location n. We extend this idea to the two-dimensional case simply by defining the basic building block of the 2D filter as $x(n_1 - k_1, n_2 - k_2)x(n_1 + k_1, n_2 + k_2)$, i.e., it consists of pixels centered around the current pixel (n_1, n_2). For the impulse response, we obtain the simple property

$$h_2(n_1, n_2, n_3, n_4) \neq 0 \text{ only if } n_1 = -n_3 \text{ and } n_2 = -n_4. \tag{8}$$

Analogous to Theorem 3, we also require that

$$\sum_{k_1}\sum_{k_2}\sum_{k_3}\sum_{k_4} h_2(k_1, k_2, k_3, k_4) = H_2(0,0,0,0) = 0. \tag{9}$$

With the symmetry of the kernel, i.e., $h_2(n_1, n_2, n_3, n_4) = h_2(n_3, n_4, n_1, n_2)$, it is also easy to prove that

$$H_2(\omega_1, \omega_2, 0, 0) = H_2(0, 0, \omega_1, \omega_2). \tag{10}$$

Using Eqs. (8), (9) and (10), we find the corresponding extension to Eq. (3) as

$$Y(\omega_1, \omega_2) \approx 2\mu_x X(\omega_1, \omega_2) H_2(\omega_1, \omega_2, 0, 0). \tag{11}$$

Assuming that $H_2(\omega_1, \omega_2, 0, 0)$ has highpass characteristics in either ω_1 or ω_2 direction or in both, we conclude that the class II two-dimensional systems can be approximated by mean-weighted highpass filters.

We only want to indicate how Eq. (11) can be proved. The exact mathematical proof follows the same idea as the proof of Theorem 1 in the appendix of this chapter. Basically, we use the general reconstruction formula for two-dimensional quadratic systems similar to Eq. (2) and substitute $X(\omega_1, \omega_2) = \hat{X}(\omega_1, \omega_2) + 4\pi^2\mu_x\delta(\omega_1, \omega_2)$, where μ_x represents the mean of $X(\omega_1, \omega_2)$. Using $H_2(0,0,0,0) = 0$, we obtain

$$Y_2(\omega_1, \omega_2) = \mathcal{V}\{\hat{X}(\omega_1, \omega_2)\} + \mu_x\hat{X}(\omega_1, \omega_2)[H_2(\omega_1, \omega_2, 0, 0) + H_2(0, 0, \omega_1, \omega_2)]. \tag{12}$$

We then show that $\mathcal{V}\{\hat{X}(\omega_1, \omega_2)\}$ contributes much less to the overall result and can thus be neglected. Resubstituting $X(\omega_1, \omega_2)$ finally yields Eq. (11).

5 Characterization of Edge Extracting Filters

5.1 Mathematical Description

In this section, we introduce a method of characterizing the isotropical behavior and the dependence of a filter output on the input frequency. Unlike in the case of linear filters, however, the influence of the input frequencies on the output spectrum is not obvious, and we cannot show this dependence in any complete and yet easily interpretable way. Even though the filter is mathematically completely defined by the frequency response $H_2(\cdot)$, a plot of this function does usually not yield any insight into the edge extracting capabilities of the system. Essentially, two factors make the analysis hard to interpret: the complexity of the system and the complexity of the input signal. Even for simple quadratic systems, the frequency domain representation can appear confusing. Above all, we cannot restrict our design to systems for which we have a simple intuitive explanation. This leaves us with the second source of complexity, the input signal. Of course, we have complete control over this for design purposes, which means that we can develop a filter that reacts in a specific way to a certain input. However, we have to make sure that the filter's response to real-world signal (i.e., arbitrary images) remains predictable. This simplification allows us to describe the behavior in more intuitive terms than by using the complete frequency response.

The choice of the input is very much determined by our design goals. The signal must be such that the system response is meaningful so that we can draw conclusion about how much we have achieved the desired behavior. To this end, we choose a single sinusoidal signal as the system input. By varying its frequency, we can roughly estimate how the systems will respond to more complex input signal with arbitrary frequency content. Even though it will

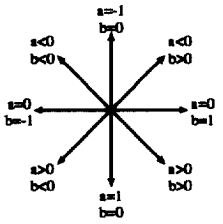

Figure 1: *Parameters a and b determine the orientation of the input sinusoid. They are interlinked by* $a^2 + b^2 = 1$.

not be possible to predict quantitatively how a system will react to an arbitrary input signal, because we do not take into consideration any intermodulation frequencies or harmonics, we still can make qualitative assertions. Since we are interested in edges and texture, and we know that in these areas the energy is mostly concentrated in the high frequency range, we approximate the result by studying the system behavior for high frequency sinusoids.

To incorporate a test for isotropy into our input signal, we use rotated sinusoids with the rotation as a free parameter:

$$x(n_1, n_2) = \sin(\omega_0(an_1 + bn_2)), \tag{13}$$

where a and b determine the orientation and $a^2 + b^2 = 1$. In Fig. 1, the possible orientations are indicated with the corresponding values for these parameters. Both must be in $[-1 \ldots 1]$ and because they are interlinked, only one of them is sufficient to define the orientation. Also, for our purposes half of the possible directions in Fig. 1 are redundant and we will only use $a \in [-1 \ldots 1]$ and $b = \sqrt{1-a^2}$.

With Eqs. (2) and (13), we compute the output spectrum. We find

$$\begin{aligned} Y_2(\omega_1, \omega_2) = \\ &\pi^2[-H_2(\omega_0 a, \omega_0 b, \omega_0 a, \omega_0 b)\delta(\omega_1 - 2\omega_0 a, \omega_2 - 2\omega_0 b) \\ &+H_2(\omega_0 a, \omega_0 b, -\omega_0 a, -\omega_0 b)\delta(\omega_1, \omega_2) \\ &+H_2(-\omega_0 a, -\omega_0 b, \omega_0 a, \omega_0 b)\delta(\omega_1, \omega_2) \\ &-H_2(-\omega_0 a, -\omega_0 b, -\omega_0 a, \omega_0 b)\delta(\omega_1 + 2\omega_0 a, \omega_2 + 2\omega_0 b)]. \end{aligned} \tag{14}$$

As expected, the output consists of components with zero and twice the input frequency. We can, however, easily show that only the DC component will be nonzero. We use Eqs. (8) and (9) and obtain

$$H_2(\omega_1, \omega_2, \omega_1, \omega_2) = \sum_{k_1} \sum_{k_2} h_2(k_1, k_2, -k_1, -k_2) = 0.$$

Thus, only the terms with $\delta(\omega_1, \omega_2)$ remain in Eq. (14) and with $Y_2^{(DC)}(\omega_0, a) = \pi^2[H_2(\omega_0 a, \omega_0 b, -\omega_0 a, -\omega_0 b) - H_2(-\omega_0 a, -\omega_0 b, \omega_0 a, \omega_0 b)]$, we have

$$Y_2(\omega_1, \omega_2) = Y_2^{(DC)}(\omega_0, a)\delta(\omega_1, \omega_2). \tag{15}$$

5.2 Graphical Representation of Example Filters

We now want to illustrate how to interpret the plots of directional and frequency dependence. We will call these graphs isotropy plots, because they indicate to which degree a filter is isotropical. In order to understand how these properties determine the system output for images, we also use an artificial image shown in Fig. 3(a). It is a ring with added Gaussian noise ($\sigma^2 = 0.01$). The image dimensions are 256×256 pixels, and the inner and outer radii of the ring are 80 and 100 pixels, respectively. Before adding the noise, pixels on the ring have unity value, outside they are zero. The step edge is almost ideal, thus containing very high frequencies, which will illustrate the differences between the filters more clearly than a smooth transition.

We define the first example system (Filter A) by the input-output relation

$$\begin{aligned} y^{(a)}(n_1, n_2) = &x^2(n_1, n_2) \\ &-x(n_1, n_2 + 1)x(n_1, n_2 - 1) \\ &-x(n_1 + 1, n_2)x(n_1 - 1, n_2) \\ &+0.5x(n_1 + 1, n_2 + 1)x(n_1 - 1, n_2 - 1) \\ &+0.5x(n_1 + 1, n_2 - 1)x(n_1 - 1, n_2 + 1). \end{aligned} \tag{16}$$

We can derive this equation by designing a system that responds with a constant output to the input signal $x(n_1, x_2) = \sin(\omega_0 n_1)\sin(\omega_0 n_2)$. The corresponding frequency responses are

$$\begin{aligned} H_2^{(a)}(\omega_1, \omega_2) = \\ (1 - \cos(\omega_1 - \omega_3))(1 - \cos(\omega_2 - \omega_4)) \end{aligned} \tag{17}$$

and

$$Y_2^{DC(a)}(\omega_0, a) = 2\pi^2(1 - \cos(\omega_0 a))(1 - \cos(\omega_0 b)). \tag{18}$$

Figure 2(a) shows the isotropy plot. The side view in (b) makes the dispersion clearly visible, i.e., we can assess to which extent the filter varies its response for different values of a.

We see that Filter A does not respond at all for $a = -1$, 0 and 1, corresponding to horizontal and vertical orientations (see Fig. 1). Comparing this to the image shown in Fig. 3(a), shows the strong directional dependence of the filter output. We can make another observation by examining the way the response rises for increasing frequencies in Fig. 2(a). For small values of ω_0, the output is very small and it starts to rise only for ω_0 greater approximately 0.5 rad. This means that the system has a strong highpass characteristic. Accordingly, the lines in Fig. 3(a) are very thin.

The second example, Filter B, is defined by

$$\begin{aligned} y^{(b)}(n_1, n_2) = &2x^2(n_1, n_2) \\ &-x(n_1 + 1, n_2)x(n_1 - 1, n_2) \\ &-x(n_1, n_2 - 1)x(n_1, n_2 + 1) \end{aligned} \tag{19}$$

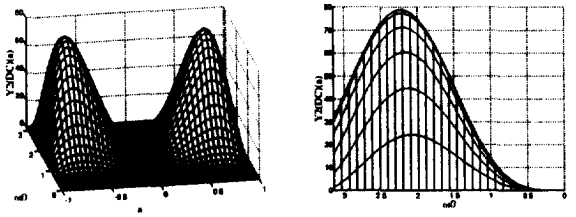

(a) Filter A

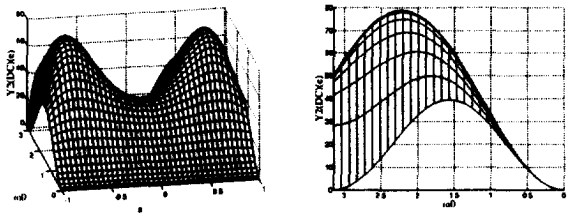

(b) Filter B

Figure 2: *Isotropy plots for the example filters. The left graph shows the regular view and the right one displays it from the side with the a-axis perpendicular the paper plane.*

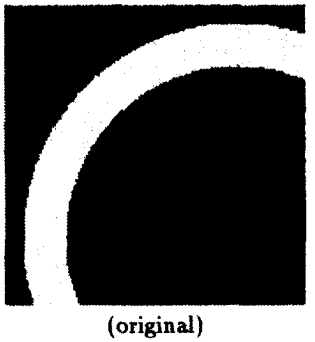

(original)

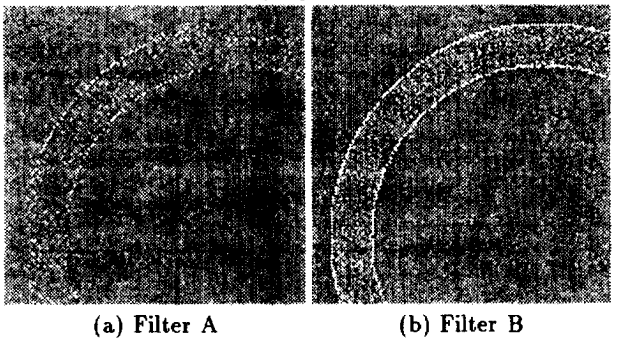

(a) Filter A (b) Filter B

Figure 3: *Original "ring" image and results of applying the example filters to it.*

$$H_2^{(b)}(\omega_1,\omega_2) = 2-\cos(\omega_1-\omega_3)-\cos(\omega_2-\omega_4) \quad (20)$$

$$Y_2^{DC(b)}(\omega_0,a) = 2\pi^2(2-\cos(2\omega_0 a) - \cos(2\omega_0\sqrt{1-a^2})). \quad (21)$$

The isotropy plot in Fig. 2(b) shows fairly isotropical behavior up to frequencies around 1 rad. Thus, it is able to extract the edges from the ring images much more evenly than Filter A. (see Fig. 3(b)).

6 Conclusions

We have investigated a subclass of one-dimensional quadratic Volterra filters, which can be written as a product of local mean and linear highpass. By extending this concept to two-dimensional systems, we could describe the general class of filters for edge extraction. To assess the differences between various filters, we have also developed an approximate description using simple two-dimensional inputs. This allows us to evaluate both the orientational dependence of the filter and its frequency characteristics and is more intuitive than the description by a four-dimensional frequency response.

References

[1] V. Volterra, *Theory of Functionals and of Integral and Integro-Differential Equations.* New York: Dover Publications, 1959.

[2] G. L. Sicuranza, "Quadratic filters for signal processing," *Proceedings of the IEEE*, vol. 80, pp. 1263 - 1285, August 1992.

[3] S. Thurnhofer, *Quadratic Volterra Filters for Edge Enhancement and Their Applications in Image Processing.* PhD thesis, University of California, Santa Barbara, 1994.

[4] S. A. Billings and K. M. Tsang, "Spectral analysis for non-linear systems, part II: Interpretation of nonlinear frequency response functions," *Mechanical Systems and Signal Processing*, vol. 3, no. 4, pp. 341 - 359, 1989.

[5] T. Vinh, T. Chouychai, H. Liu, and M. Djouder, "Second order transfer function: Computation and pysical interpretation," in *Proc. SPIE International Modal Analysis Conf.*, (London, UK), pp. 587 - 592, 1987.

[6] H. Zhang, *Frequency Domain Estimation and Analysis for Nonlinear Systems.* PhD thesis, University of Sheffield, 1993.

[7] J. F. Kaiser, "On a simple algorithm to calculate the 'energy' of a signal," in *Proc. IEEE Intl. Conf. on Acoustics, Speech & Signal Processing*, (Albuquerque, NM), pp. 381 - 384, April 1990.

[8] S. K. Mitra, H. Li, I. S. Lin, and T.-H. Yu, "A new class of nonlinear filters for image enhancement," in *Proc. IEEE Intl. Conf. on Acoustics, Speech & Signal Processing*, (Toronto, Canada), pp. 2525 - 2528, 1991.